Available online at www.sciencedirect.com

ScienceDirect

journal homepage: www.elsevier.com/locate/he

Theoretical study of hydrogen adsorption kinetics: $Mg_{17}Al_{12}$ vs pure Mg

Xingyu Zhou [a], Xiaotong Yan [a], Changchun He [a], Xiao-Bao Yang [a], Yu-Jun Zhao [a,b,*]

[a] Department of Physics, South China University of Technology, Guangzhou, 510640, China
[b] Key Laboratory of Advanced Energy Storage Materials of Guangdong Province, South China University of Technology, Guangzhou, 510640, China

HIGHLIGHTS

- Hydrogen adsorption on $Mg_{17}Al_{12}$ surfaces are stronger than Mg(0001) surface.
- H_2 dissociation barriers of $Mg_{17}Al_{12}$ surfaces are lower than Mg(0001) surface.
- H atoms obtain similar charges on the $Mg_{17}Al_{12}$(110) and Mg(0001) surfaces.
- The stronger hybridization of H s and Al s orbitals enhances H_2 dissociation.

GRAPHICAL ABSTRACT

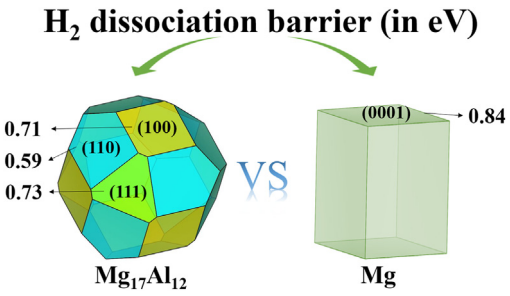

ARTICLE INFO

Article history:
Received 21 November 2022
Received in revised form
9 January 2023
Accepted 23 January 2023
Available online 16 February 2023

Keywords:
Hydrogen dissociation
Hydrogen adsorption
Kinetics
First-principles calculation

ABSTRACT

The adsorption and dissociation of hydrogen molecules on $Mg_{17}Al_{12}$(100), $Mg_{17}Al_{12}$(110), $Mg_{17}Al_{12}$(111) and Mg(0001) surfaces are investigated by the first-principles calculations. We find that the H adsorption on $Mg_{17}Al_{12}$ systems are all stronger than that of Mg(0001). Among them, the lowest adsorption energies of H atoms are obtained in the $Mg_{17}Al_{12}$(110) system, which is −0.278 and −0.247 eV/H when the H coverage is 1/11 and 2/11 ML, respectively. Furthermore, the $Mg_{17}Al_{12}$(110) surface presents an energy path of hydrogen dissociation with a minimum barrier of 0.59 eV, which is smaller than that of Mg(0001) surface (0.84 eV). The electronic structure analysis illustrates that the bonding between H atoms and $Mg_{17}Al_{12}$(110) surface is enhanced, although H atoms obtain similar charges on the $Mg_{17}Al_{12}$(110) and Mg(0001) surfaces. Moreover, the lowered dissociation barrier on the three studied $Mg_{17}Al_{12}$ surfaces, are likely ascribed to the stronger hybridization of H 1s and Al 3s orbitals, leading to the accelerated hydrogen adsorption kinetics on $Mg_{17}Al_{12}$ surface with respect to the pure Mg surface.

* *Corresponding author*. Department of Physics, South China University of Technology, Guangzhou, 510640, China.
E-mail address: zhaoyj@scut.edu.cn (Y.-J. Zhao).

https://doi.org/10.1016/j.ijhydene.2023.01.273
0360-3199/

Introduction

Hydrogen is an ideal new energy source for automobiles, because it is not only lightweight, highly abundant, environmentally friendly, recyclable, but also has a high combustion calorific value [1–3]. In the application of hydrogen energy, the storage of hydrogen is critical. While researching how to store hydrogen safely, scientists have found that solid-state storage systems based on metal hydrides are highly promising due to their high safety, high hydrogen storage density, and reversible hydrogen absorption and desorption [2–10]. Especially, MgH_2 has attracted various interests due to its high storage capacity (7.6 wt% H_2) and low price [9,10]. However, further improvement is required before it meets the market application needs [11].

Many efforts have been made to improve the hydrogen storage properties of MgH_2, both thermodynamically and kinetically, the addition of a catalytic metal is believed to improve the hydrogen absorption properties [12–19]. Al element is considered due to its similar physical properties [12,15,20–32]. Bououdina *et al.* [21] prepared Mg:Al (90:10, 75:25, 58:42, 37:63, 20:80) alloys in their high-energy ball milling and Al-leaching forms, found that Al acts essentially as a diluent and does not decrease the hydrogen absorption capacities of Mg significantly in the materials. There is an improvement in the kinetics of hydrogen absorption and desorption following Al leaching. Moreover, the adding of 0.8 mol Al into 1.0 mol MgH_2 gives the second fastest dehydrogenation kinetics after Ni at 300 °C under vacuum, compared with Fe, Nb, Ti and Cu [12]. A series of researches by Crivello *et al.* [22,26] also claimed that Al promotes to destabilize MgH_2 by forming the two Mg–Al alloys, β-Mg_2Al_3 and γ-$Mg_{17}Al_{12}$. Al-based phases should be the key factor which controls the thermodynamics properties of hydrogenation. Further study [33] found that the substitution of Al for Mg in MgH_2 weakens the interaction between Mg and H atoms and has a high potential to drive the formation of Al–Mg clusters. The extra electrons occupy the minimum of the conduction band so that the band gap could disappear when Al atoms are doped at Mg sites. Consequently, the stepwise removal of H_2 molecules from Al-substituted MgH_2 is much easier than the pure MgH_2 [34]. Andreasen [25] announced that improved kinetics were generally found in the hydrogenation and dehydrogenation of Mg–Al alloy.

Since the addition of Al has a positive effect on the hydrogen storage properties of MgH_2, the stable Mg–Al phase (γ-$Mg_{17}Al_{12}$) with 4.4 wt% hydrogen content, has reversible hydrogen absorption and desorption reaction, attracting interests from scientists [20,22,24,25,28,30]. However, it is still unclear why the hydrogen absorption kinetics of $Mg_{17}Al_{12}$ is faster than that of pure Mg. What is the role of Al in the promotion of hydrogen absorption kinetics? It is clear that hydrogen absorption consists of the following procedure: firstly, hydrogen molecules are adsorbed on the surface, then dissociated into two hydrogen atoms, and finally hydrogen atoms diffuse on the surface or enter the interior of the bulk phase [35].

Here, we have selected its three low-index surfaces (100), (110) and (111) for hydrogen adsorption investigation based on the three major X-ray diffraction peaks of $Mg_{17}Al_{12}$ [23]. The microscopic mechanism of hydrogen adsorption, dissociation, and sticking on the $Mg_{17}Al_{12}$(100), (110) and (111) surfaces are theoretically studied, by employing first-principles calculations. The above calculation is also performed for Mg(0001) surface to be a comparison. As a result, the kinetics of hydrogen adsorption on the surfaces of $Mg_{17}Al_{12}$(100), $Mg_{17}Al_{12}$(110) and $Mg_{17}Al_{12}$(111) are revealed to be faster than that of Mg(0001) by a series of analytical means, especially for the $Mg_{17}Al_{12}$(110) system. It is demonstrated that the kinetic improvement is attributed to the presence of Al in the $Mg_{17}Al_{12}$ alloy.

Methods

All total-energy calculations of bulk $Mg_{17}Al_{12}$, the three low-index surfaces of $Mg_{17}Al_{12}$ and Mg(0001) surface with and without hydrogen atoms were performed using Vienna *ab* initio simulation package (VASP) [36] based on density functional theory (DFT). The generalized gradient approximation (GGA) [37] of Perdew, Burke, and Ernzerhof (PBE) [38] was adopted to elaborate exchange-correlation function. The criteria for convergence of electronic states and Hellmann-Feynman forces were set to 1×10^{-6} eV and 0.01 eV/Å, respectively. The cutoff energy was set to 520 eV and Monkhorst-Pack special k-point scheme [39], $3 \times 3 \times 3$ and $3 \times 3 \times 1$ (or $2 \times 2 \times 1$) *k*-point grids were used for bulk and slab systems. In all slab systems, the lower half of the atomic layer was fixed and the other half was relaxed. Activation energies have been calculated using the climbing image nudged elastic band (CI-NEB) method [40] to find the minimum energy path of hydrogen dissociation.

Results and discussion

Structural stability

$Mg_{17}Al_{12}$ ($I\bar{4}3m$, group no. 217) contains 17 Mg and 12 Al atoms in a primitive cell. The optimized lattice parameters of $Mg_{17}Al_{12}$ are $a = b = c = 10.53$ Å for the conventional cell, very close to the experimental values [25]. The three low-index surfaces, actually have various possible terminations. Here we have singled out the stable terminations of (100), (110) and (111) surfaces from the mostly possible terminals by their structure regularity and stoichiometry. In detail, 4, 3, 4 terminals, with 8, 6, 8 atomic layers, are considered for $Mg_{17}Al_{12}$(100), (110) and (111) surfaces, respectively, as shown in Fig. 1(a–c). The surface energy is a good value to reflect the stability of various terminals. Here, the surface energies of different terminations for $Mg_{12}Al_{17}$(100), (110) and (111) are calculated using the following formulas [41,42]:

$$\sigma_{Mg-Al}^{slab} = \frac{1}{2A}\left(E_{slab}^{unrelax} - \frac{N_{Al}^{slab}}{N_{Al}^{bulk}}\mu_{Mg-Al}^{bulk}\right) + \frac{1}{A}\left(E_{slab}^{relax} - E_{slab}^{unrelax}\right) \quad (1)$$

Where *A* is the surface area of the slab, N_{Mg}^{slab} (N_{Al}^{slab}) and N_{Mg}^{bulk} (N_{Al}^{bulk}) are the number of Mg (Al) atoms of the slab (see Table 1) and bulk. $E_{slab}^{unrelax}$ and E_{slab}^{relax} is the total energy of the slab before

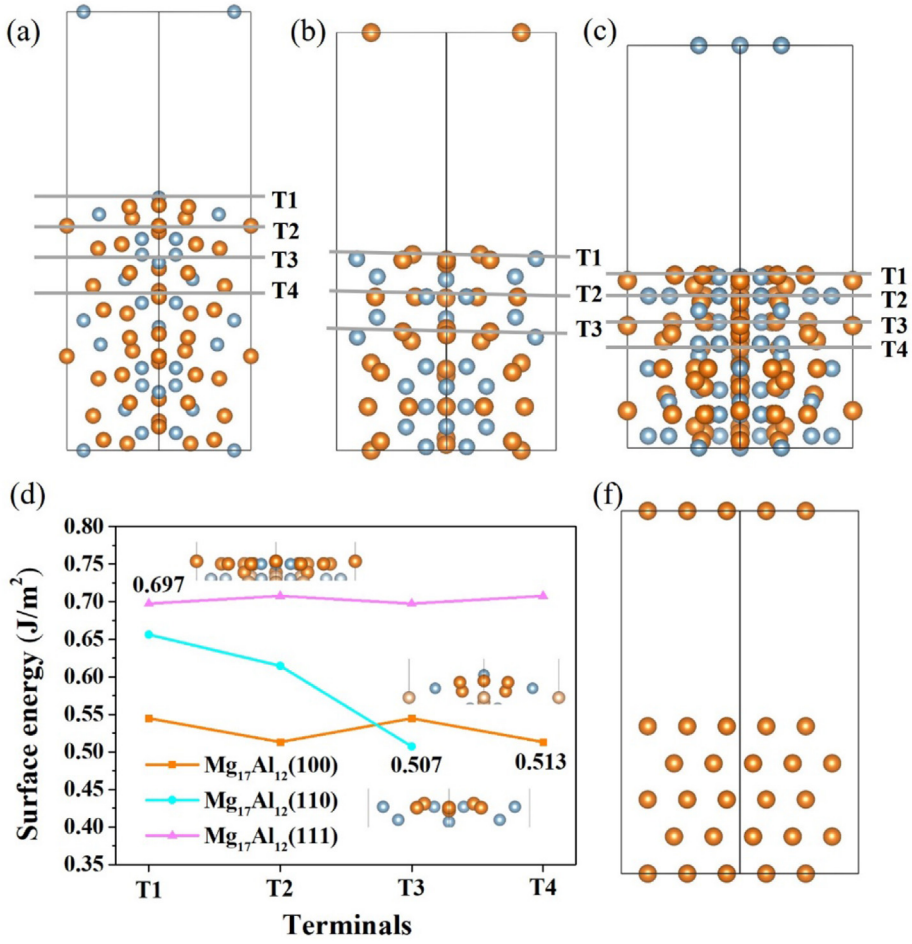

Fig. 1 – The slabs of (a) $Mg_{17}Al_{12}$(100), (b) $Mg_{17}Al_{12}$(110), (c) $Mg_{17}Al_{12}$(111) cleaved form $Mg_{17}Al_{12}$ conventional cell. T1, T2, T3 and T4 refer to different terminals in the slabs. (d) Surface energy varies by terminations. T4, T3, T1 of the (100), (110), (111) slabs with the lowest surface energy are selected. (f) The slab of Mg(0001) surface with 5 layers. Color legend: Mg, orange; Al, blue. (For interpretation of the references to color in this figure legend, the reader is referred to the Web version of this article.)

Table 1 – Calculated lattice parameters and E_{form}^{slab} of $Mg_{17}Al_{12}$(100), (110), (111) slabs and Mg(0001) slab.

slab	N_{Mg}^{slab}	N_{Al}^{slab}	a (Å)	b (Å)	angles (degrees)	E_{form}^{slab} (eV/atom)
$Mg_{17}Al_{12}$(100)	68	48	10.531	10.531	$\gamma = 90.00$	0.068
$Mg_{17}Al_{12}$(110)	34	24	9.120	9.120	$\gamma = 70.53$	0.093
$Mg_{17}Al_{12}$(111)	68	48	14.893	14.893	$\gamma = 120.00$	0.154
Mg(0001)	45	0	9.569	9.569	$\gamma = 120.00$	0.124

and after relaxing, respectively. $\mu_{Mg_{17}Al_{12}}^{bulk}$ are the chemical potentials corresponding to bulk $Mg_{17}Al_{12}$. The calculated surface energy is presented in Fig. 1(d). As shown in Fig. 1(d), it indicates that the T4, T3, T1 is the most stable terminations for the $Mg_{17}Al_{12}$(100), (110) and (111) surfaces with 0.513, 0.507, 0.697 J/m^2, and the (110) as the most stable surface, in line with the experimental report [43]. For the Mg(0001) surface, a (3 × 3) slab model containing 45 Mg atoms is employed as shown in Fig. 1(f), which has 5 atomic layers along the c direction with a vacuum of 15 Å.

To identify the relative stability of the three low-index surfaces of $Mg_{17}Al_{12}$ comparing to the Mg(0001) slab, the formation enthalpy is estimated via definition

$$E_{form}^{slab} = \left(E_{slab}^{relax} - N_{Mg}^{slab}\mu_{Mg}^{bulk} - N_{Al}^{slab}\mu_{Al}^{bulk}\right) \Big/ \left(N_{Mg}^{slab} + N_{Al}^{slab}\right) \quad (2)$$

The formation enthalpy of pure Mg(0001) slab is 0.124 eV/atom (c.f. Table 1), higher than that of $Mg_{17}Al_{12}$(100) and $Mg_{17}Al_{12}$(110) slabs, but lower than $Mg_{17}Al_{12}$(111) slab. Therefore, the $Mg_{17}Al_{12}$(100) and $Mg_{17}Al_{12}$(110) slabs are energetically favorite to be formed comparing to the Mg(0001) slabs.

Hydrogen adsorption

In order to obtain the dissociation paths of H_2 molecules, the adsorption model of one H_2 molecule and that of two H atoms

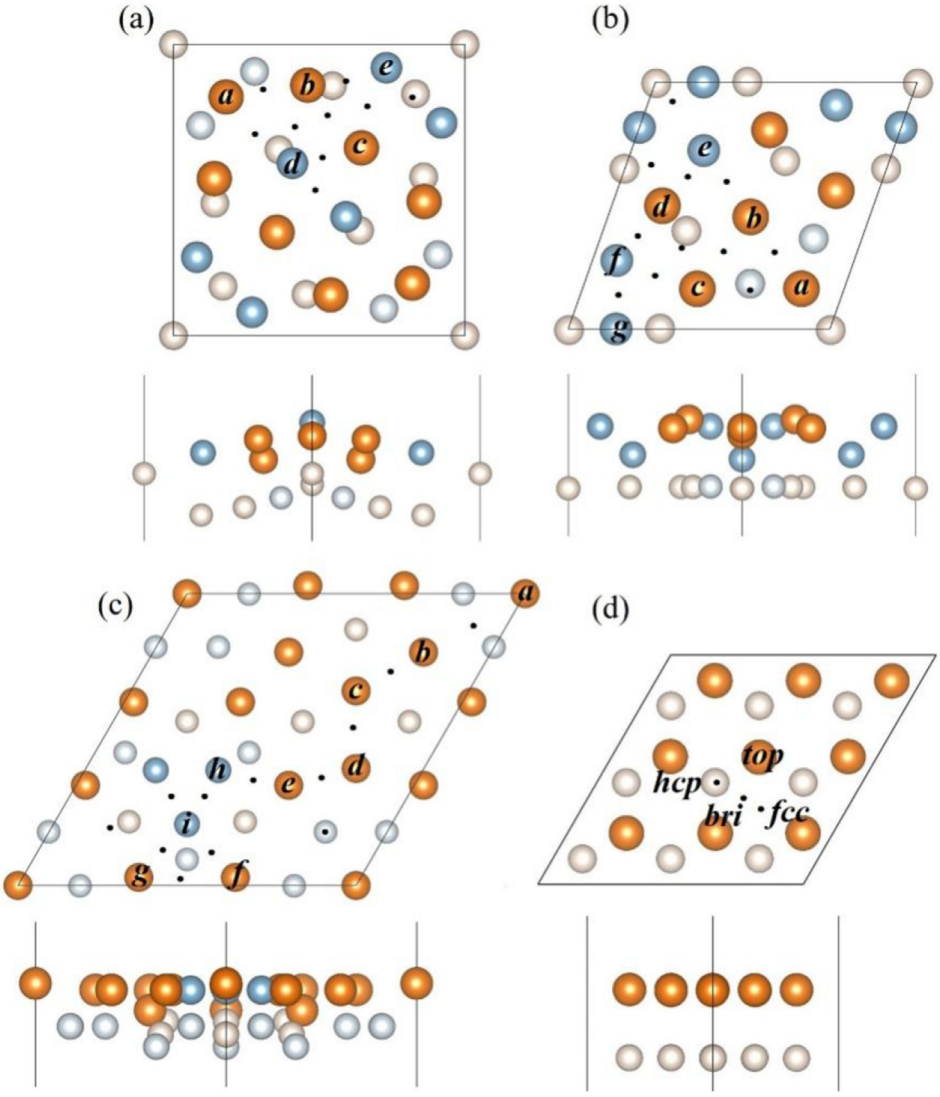

Fig. 2 – Possible adsorption sites for H atoms and H_2 molecule on (a) $Mg_{17}Al_{12}$(100) slab, (b) $Mg_{17}Al_{12}$(110) slab, (c) $Mg_{17}Al_{12}$(111) slab, (d) Mg(0001) slab. The top and bottom panels illustrate the top view and side view, respectively. Color legend: Mg, orange; Al, blue; Mg (Al) below the termination, light orange (blue). (For interpretation of the references to color in this figure legend, the reader is referred to the Web version of this article.)

need to be used as the initial and final states, respectively. The adsorption model for two H atoms is obtained by searching for the preferred adsorption sites of single H atom. As there are 14, 11, 14 and 9 atoms in the selected terminals of $Mg_{17}Al_{12}$(100), (110), (111) and Mg(0001) systems, respectively. The coverage of the adsorption model for the single H atom was 1/14, 1/11, 1/14, and 1/9 ML (stands for monolayer, a unit of coverage) for the $Mg_{17}Al_{12}$(100), (110), (111) and Mg(0001) systems, respectively. The coverage is doubled in the adsorption system of two H atoms. Selected atomic adsorption sites for the single H adatom and H_2 on $Mg_{17}Al_{12}$(100), (110), (111) surfaces and Mg(0001) are shown in Fig. 2(a) and (b), 2(c) and 2(d), respectively. For $Mg_{17}Al_{12}$(100), the top sites of *a* to *e* and the bridge site between these are considered. As for (110) and (111) surfaces, the corresponding atop sites are *a* ~ *g* and *a* ~ i, respectively. As for the adsorption sites of hydrogen on the Mg(0001) surface, there has been a lot of research [44,45], thus the same sites, *hcp*, *fcc*, *top*, *bri*, are repeated in this work as shown in Fig. 2(d). The adsorption energies of H atom (H_2 molecule) on these adsorption sites are employed for the preferred adsorption sites. The adsorption energy was defined as $E_{ads} = E_{slab+adsorbate} - E_{slab} - E_{adsorbate}$, where $E_{slab+adsorbate}$, E_{slab}, and $E_{adsorbate}$ are the total energies of the surface with adsorbate, of the bare surface, and of adsorbate, while $E_H = 1/2E_{H_2}$, *i.e.*, corresponding to the H-rich condition. E_{H_2} represents the energy of the isolated H_2 molecule, which is calculated in a large box of $10 \times 11 \times 12$ Å^3.

The adsorption sites with negative adsorption energies are shown in Fig. 3. For the $Mg_{17}Al_{12}$(100) surface, total adsorption energy calculations indicate that the H atom with the coverage of 1/14 ML is deviated to adsorb at the bridge site as shown in Fig. 3(a). The H atoms in the preferred adsorption sites are all bonded to the Al atoms. The lowest adsorption energy (−0.176 eV/H) is obtained when the H atom is adsorbed between

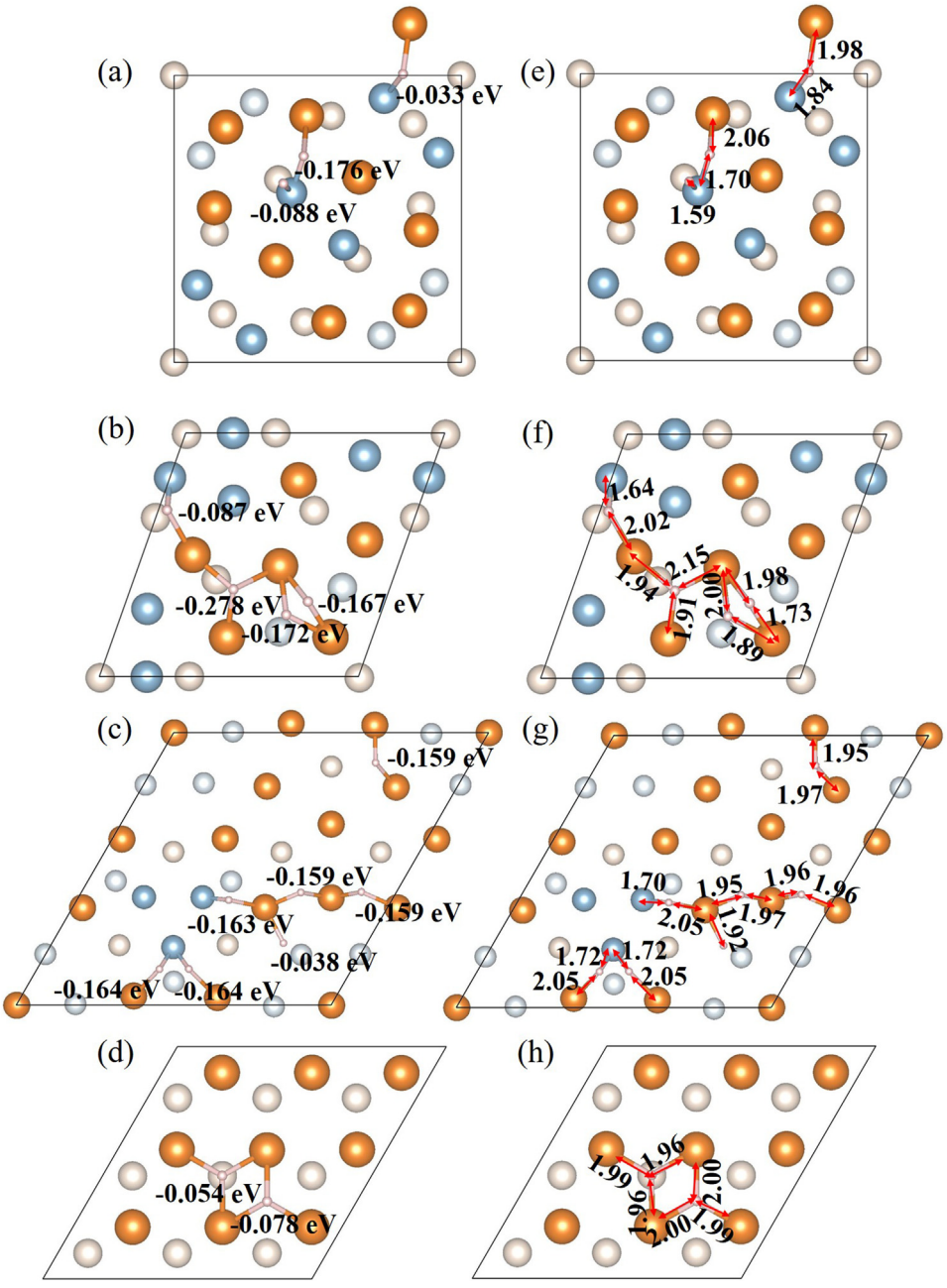

Fig. 3 – Preferred adsorption sites for single H atom on the (a) $Mg_{17}Al_{12}$(100), (b) $Mg_{17}Al_{12}$(110), (c) $Mg_{17}Al_{12}$(111) and (d) Mg(0001) surface with negative adsorption energies (in eV), and the bond lengths (in Å) of H–Mg (H–Al) are marked in (e), (f), (g), (h). Color legend: Mg, orange; Al, blue; H, light pink; Mg (Al) below the termination, light orange (blue). (For interpretation of the references to color in this figure legend, the reader is referred to the Web version of this article.)

the Mg and Al atoms with distances of 2.06 and 1.70 Å, respectively. In the $Mg_{17}Al_{12}$(100) system with H coverage of 2/14 ML, the model with lowest adsorption energy (−0.219 eV/H) is considered as the final state for the dissociation of the H_2 molecule. Here one H is adsorbed on the site with the lowest adsorption energy, while the other is adsorbed on another equivalent site. When the H atom is adsorbed on the $Mg_{12}Al_{17}$(110) surface at a coverage of 1/11 ML, it is more preferentially adsorbed at the interstitial and bridge sites between Mg atoms, as shown in Fig. 3(b). The most stable site (−0.278 eV/H) appears to be at the interstitial site among three Mg atoms in the (110) system. We have considered all the possible combination of two H adsorption configurations for the adopted slab model, *i.e.*, a coverage of 2/11 ML. It reveals that the most stable one (−0.277 eV/H) is with one H atom at the bridge site between *a* and *d*, and the other at the interstitial site among *b*, *c* and *d*.

As demonstrated in Fig. 3(c, g), in the $Mg_{17}Al_{12}$(111) system with H coverage of 1/14 ML, the adsorption energies of H atoms adsorbed on multiple bridge sites between Mg and Mg, Mg and Al are similar, tending to −0.164 eV and −0.159 eV, respectively. The bond length of Mg–H varies from 1.95 to 2.05 Å, while that of the Al–H bond is about 1.72 Å. This

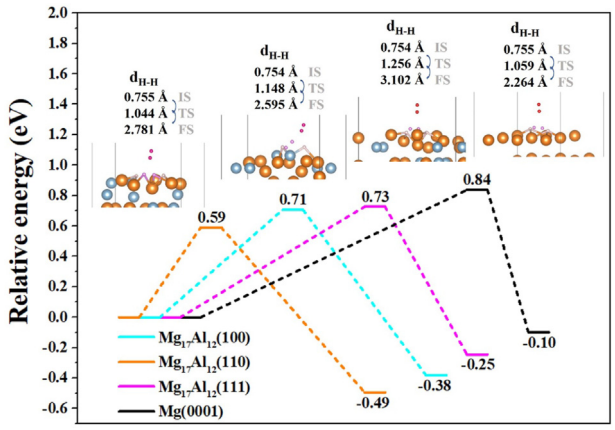

Fig. 4 – MEPs of H_2 dissociation on the $Mg_{17}Al_{12}$(100), $Mg_{17}Al_{12}$(110), $Mg_{17}Al_{12}$(111), Mg(0001) surfaces. The energy barrier of hydrogen dissociation on the $Mg_{17}Al_{12}$(110) surface is the lowest.

surface has the most preferred adsorption sites, and the model with double H, *i.e.* coverage of 2/14 ML, is correspondingly the most abundant, although the lowest adsorption energy of the two-atom adsorption model is −0.203 eV/H. The models of two different coverage of H for the three low-index surfaces of $Mg_{17}Al_{12}$ is obtained, followed by the well investigated Mg(0001) system. According to Fig. 3(d, h), the H atoms of all four preset adsorption sites (*top*, *bri*, *fcc*, *hcp*) migrate to the *hcp* site (−0.054 eV/H) and the *fcc* site (−0.078 eV/H) after optimization when H coverage is at 1/9 ML.

The most stable site for H atom adsorb on Mg(0001) surface is at *fcc* site, with adsorption energy of −0.078 eV/H, in line with the reported −0.080 eV/H [44], −0.076 eV/H [46]. Compared to −0.219 eV/H for $Mg_{17}Al_{12}$(100), −0.277 eV/H for $Mg_{17}Al_{12}$(110), and −0.203 eV/H for $Mg_{17}Al_{12}$(111), the adsorption energy of the Mg(0001) system with H coverage of 2/9 ML is the largest (−0.074 eV/H). Moreover, the adsorption energies of H_2 molecule on the $Mg_{17}Al_{12}$ surfaces and the Mg(0001) system are not much difference, around −0.040 to −0.110 eV/H_2. Overall, Fig. 3 shows that the bond length of Mg–H is roughly between 1.73 and 2.05 Å, while that of Al–H is around 1.59 to 1.72 Å. When H atom is bonded with Mg and Al atoms at the same time, the adsorption energy of H atom is lower than that of bonding alone. Besides, the lowest adsorption energies of single and double H atoms on $Mg_{17}Al_{12}$(100), (110) and (111) surfaces are all lower than that of Mg(0001) system. Overall, $Mg_{17}Al_{12}$(110) surface has the lowest H adsorption energy, followed closely by the (100) and (111) surfaces.

Hydrogen molecule dissociation

As the adsorption model of the one H_2 molecule and two H atoms are obtained, the possible hydrogen molecule dissociation paths are searched here. The minimum energy paths (MEPs) and activation barriers of H_2 dissociation over the various low-index surfaces of $Mg_{17}Al_{12}$ and Mg(0001) surface, are described in Fig. 4. It is clear that the order of magnitude of the dissociation barrier for the MEPs is: $Mg_{17}Al_{12}$(110) < $Mg_{17}Al_{12}$(100) < $Mg_{17}Al_{12}$(111) < Mg(0001), which means that the hydrogen adsorption kinetics of $Mg_{17}Al_{12}$ is faster than that of pure Mg, consistent with the experimental observations [25].

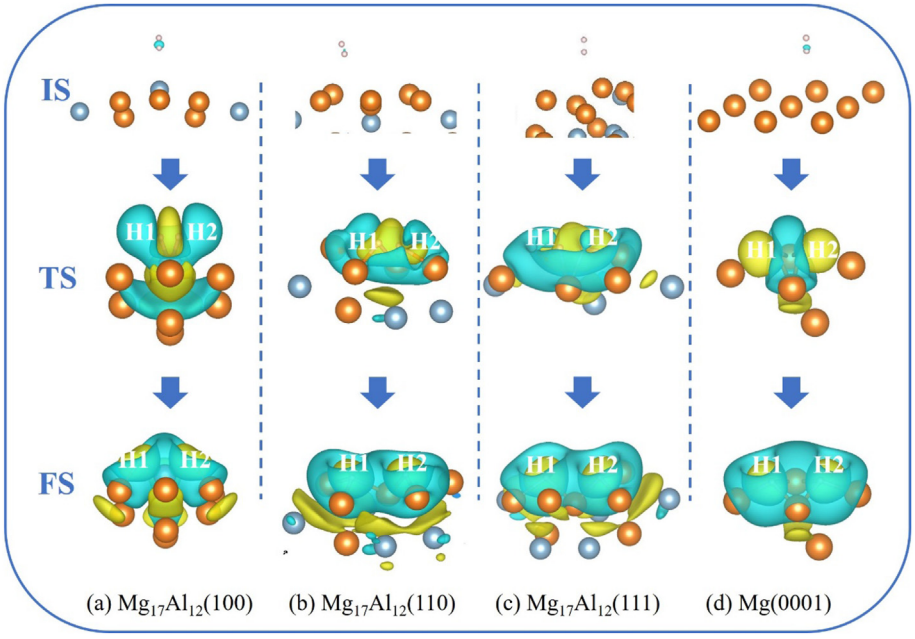

Fig. 5 – The charge density difference of H_2 dissociation on the (a) $Mg_{17}Al_{12}$(100), (b) $Mg_{17}Al_{12}$(110), (c) $Mg_{17}Al_{12}$(111), (d) Mg(0001) surfaces in the IS, TS and FS. The yellow and blue isosurfaces indicating charge accumulation and charge depletion regions, respectively. Isosurface charge density is taken to be 7×10^{-4} e/Bohr^3. (For interpretation of the references to color in this figure legend, the reader is referred to the Web version of this article.)

The calculated barrier of MEP on the Mg(0001) is 0.84 eV, similar to the earlier reported results of 0.87 eV [47] and 0.85 eV [44]. The hydrogen molecules gradually approached the surface, and the two hydrogen atoms also gradually pulled apart due to the attraction of the surface Mg atoms, ranging from 0.755 to 1.059 to 2.264 Å, and the two H atoms were finally adsorbed at the *hcp* and *fcc* sites on the Mg(0001) surface, respectively. For the $Mg_{17}Al_{12}$(100), (110) and (111) surfaces, the images at the initial state (IS) are similar. The H–H dimer is perpendicular to the slab with a H–H bond of ~0.755 Å, away from the surface. Subsequently, the H–H dimers gradually descended to the surfaces and the two hydrogen atoms gradually pulled apart, reaching a distance of 1.148, 1.044, 1.256 Å in the transition state (TS) on $Mg_{17}Al_{12}$(100), (110) and (111) surfaces, respectively. It is confirmed that the structures of TS have only one imaginary frequency, which are 1199.56, 821.71 and 1025.01 cm^{-1} for the three surfaces, respectively. In the final state (FS), the two H atoms on the $Mg_{17}Al_{12}$(100) surface are both adsorbed between the Mg and Al atoms to form Mg–H–Al bond, respectively. This is different from the H atoms on $Mg_{17}Al_{12}$(110) and (111) surface, which are both firmly bonded to its nearest Mg atoms. In addition, for the $Mg_{17}Al_{12}$(100), (110) and (111) surfaces, the energy difference between FS and IS are −0.38, −0.49, −0.25 eV, respectively, during the dissociation of the hydrogen molecule.

Electronic structure analysis

In order to understand why the H_2 molecule dissociation barrier of $Mg_{17}Al_{12}$ surfaces are smaller than that of pure Mg surface, the differential charge density and projected density of states (PDOS) of $Mg_{17}Al_{12}$ and pure Mg surfaces are present in Figs. 5 and 6. The PDOS of Mg and Al atoms with remarkable charge transfer are selected out based on the differential charge density. The Mg (Al) orbitals presented in Fig. 6 is the sum of the PDOS of all the Mg (Al) atoms involved in the reaction.

Fig. 5 shows that there is no chemical interaction between the H_2 molecule and the metal surfaces in the IS. The charge of H1 and H2 atoms in all systems listed in Table 2 are all around

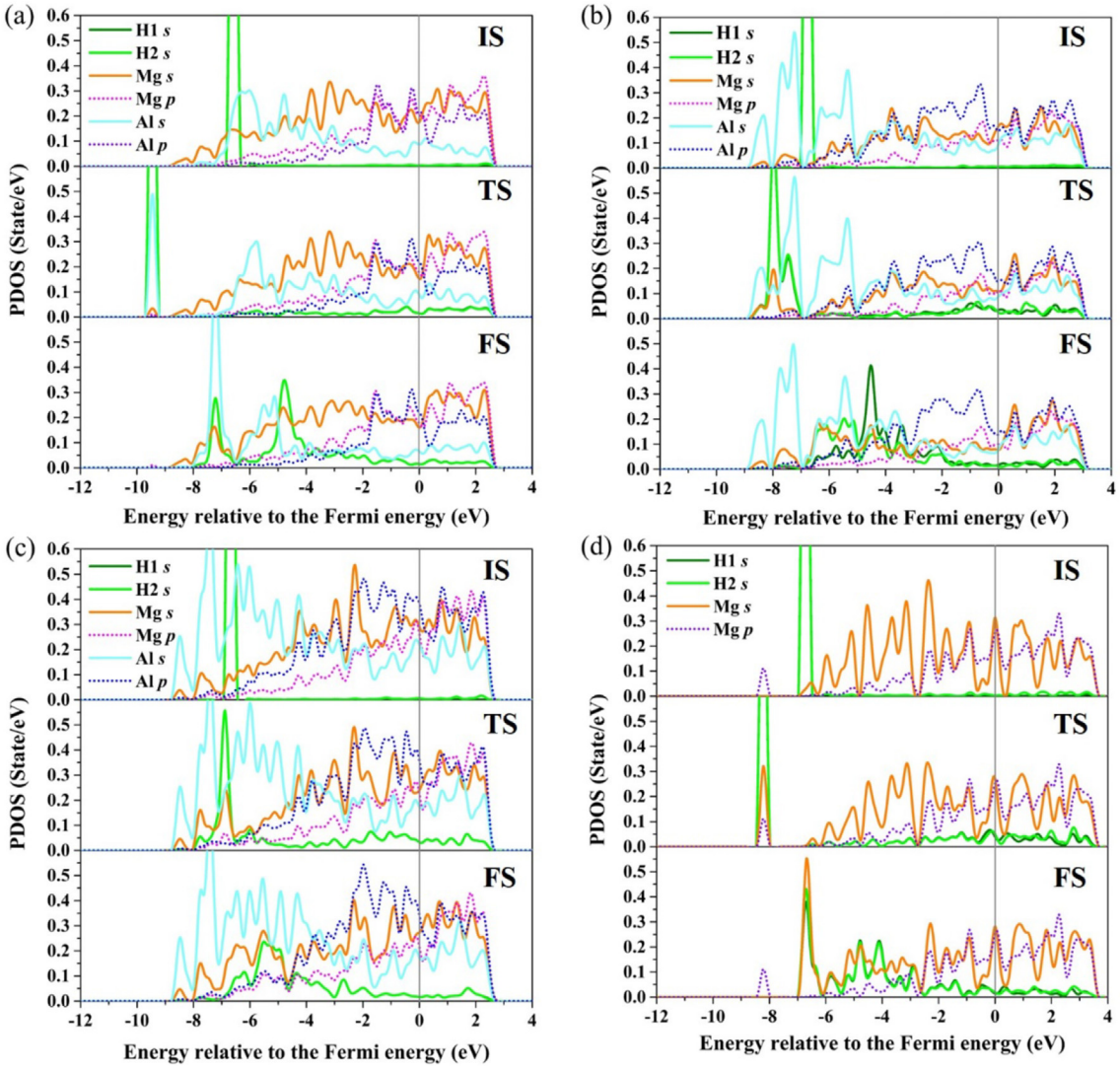

Fig. 6 – PDOS of two H atoms and their immediate neighbors on the (a) $Mg_{17}Al_{12}$(100), (b) $Mg_{17}Al_{12}$(110), (c) $Mg_{17}Al_{12}$(111), (d) Mg(0001) surfaces in the IS, TS and FS.

Table 2 – The Bader charge (in *e*) of the H1 and H2 (after the slash) atoms for the $Mg_{17}Al_{12}$(100), (110), (111) systems and Mg(0001) system, respectively, in the IS, TS, and FS.

State/system	$Mg_{17}Al_{12}$(100)	$Mg_{17}Al_{12}$(110)	$Mg_{17}Al_{12}$(111)	Mg(0001)
IS	1.04/0.99	1.03/1.01	1.00/1.04	1.00/1.05
TS	1.24/1.24	1.54/1.57	1.66/1.65	1.57/1.67
FS	1.82/1.82	1.84/1.91	1.94/1.94	1.95/1.97

1.00 *e* per H, indicating that there is negligible charge transfer from the metal surface to the H_2 molecule. In the TS, both H1 and H2 atoms on $Mg_{17}Al_{12}$(100) are bonded to the Al atom on the surface, while H atoms gain electrons from the Al atom, which also gains electrons form the nearby atoms. At the same time, the charge of H1 and H2 are the same, both being 1.24 *e*, reflecting H1 and H2 occupy two equivalent adsorption sites. The H1 and H2 atoms in the $Mg_{17}Al_{12}$(110) system bond only with Mg and gain electrons from the neighbor Mg atoms. Moreover, the electrons lost by these Mg atoms are given not only to the H atoms but also to the subsurface Al atom by a small part. The obtained electrons of the two H atoms in the $Mg_{17}Al_{12}$(110) system are twice as that in the $Mg_{17}Al_{12}$(100) system.

Compared with the three $Mg_{17}Al_{12}$(100) and (110) system, the (111) system has the largest value of charges, 1.66 *e* for H1 and 1.65 *e* for H2, in the TS. Furthermore, the electrons H atoms obtained in the Mg(0001) system are only from two Mg atoms. This may be attributed to fact that the average valence charge of Mg atoms in the free Mg(0001) surface is 2.00 *e*, while it is only about 1.00 *e* in $Mg_{17}Al_{12}$ system. This reflects that there are significant charge transfers from Mg to Al. In the FS, H atoms obtain a large number of electrons from the nearby atoms of the four metal surfaces and forms some strong bonds with Mg or Al atoms. The charges of H1/H2 in the $Mg_{17}Al_{12}$(100), (110), (111) systems and Mg(0001) system in FS are 1.82/1.82, 1.84/1.91, 1.94/1.94, 1.95/1.97 *e*, respectively. It is obvious that when a hydrogen molecule dissociates into two H atoms and then chemisorbed on the metal surfaces, the two hydrogen atoms can gain 0.82 to 0.97 *e* per H from the surface, respectively. It can be speculated that the bonding between the two H atoms and the three surfaces of $Mg_{17}Al_{12}$ are stronger than that of pure Mg(0001) system. This is due to the reduced charge value of the Mg atoms in the former system. As a result, the adsorption energies of the $Mg_{17}Al_{12}$(110) systems in the TS and FS are much lower than that of pure Mg(0001) when H atoms gain about the same number of charges from the metal surfaces.

In the IS, the H_2 molecule is still far from the metal surface and there is no overlap between the H_2 molecule orbitals and the orbitals of the $Mg_{17}Al_{12}$ and pure Mg surfaces as shown in Fig. 6. The main peaks of the hydrogen molecule orbitals of the IS for the $Mg_{17}Al_{12}$(100), (110), (111) and Mg(0001) surfaces are all around −6.7 eV. At the TS, instead, there is a clear interaction between the H 1*s* orbital and the orbitals of the surface metal atoms in both $Mg_{17}Al_{12}$ and pure Mg systems when gaseous hydrogen has started dissociating over the surface. In addition, not only the position of the H 1*s* orbit seems to have a significant negative shift during the transition from IS to TS, the magnitude of the H 1*s* peak under the Fermi level is also reduced. This is consistent with the calculations by Pozzo *et al.* [47] on the hydrogen dissociation of Mg(0001) system. Among them, the peak of the H 1*s* orbital of the $Mg_{17}Al_{12}$(110) system not only shifts to the lower energy, but also split into two peaks at transition state. The main peak overlaps with the Mg *s* orbital and the secondary peak overlaps with the Al 3*s* orbital. The distributions of main bonding peaks of are concentrated in the energy region of −8.0 to −7.5 eV. On the contrast, the overlap area of H 1*s* orbitals and Al 3*s* orbitals in the $Mg_{17}Al_{12}$(100) system is larger than that of H 1*s* orbitals and Mg 3*s* orbitals. Overall, the H 1*s* orbitals of $Mg_{17}Al_{12}$ and pure Mg systems are shifted positively toward to the Fermi level from the TS to FS. In the FS, several peaks appear in the H 1*s* orbitals in all systems, and the peaks also shift towards the Fermi level. Unlike the $Mg_{17}Al_{12}$(100) and Mg(0001) systems, the orbitals of the H1 1*s* and H2 1*s* in the $Mg_{17}Al_{12}$(110) system no longer completely overlap. Interestingly, the Al 3*s* orbitals in all three $Mg_{17}Al_{12}$ systems show a remarkable change when overlapping with H 1*s* orbital in the TS. Moreover, the main peaks of Al 3*s* orbitals are closer to H 1*s*, which facilitates the overlap of Al 3*s* and H 1*s* orbitals. This likely leads to the fact that the hydrogen dissociation barrier energies of the MEPs of the three $Mg_{17}Al_{12}$ systems are all lower than Mg(0001) system.

Conclusions

In summary, the structural and electronic characteristics of Mg(0001) surface and (100), (110) and (111) surfaces of $Mg_{17}Al_{12}$ alloy on hydrogen adsorption are studied with the first-principles calculations. Through the calculation of surface energy, the terminations with the lowest corresponding surface energy for $Mg_{17}Al_{12}$(100), (110) and (111) surfaces respectively are selected to investigate the kinetic process of hydrogen adsorption and dissociation. It is revealed that the adsorption of H atoms on $Mg_{17}Al_{12}$(100), (110) and (111) surfaces are all stronger than that on Mg(0001). The hydrogen dissociation barriers of these three low-index surfaces of $Mg_{17}Al_{12}$ are all smaller than Mg(0001) system, implying that the kinetics of hydrogen adsorption on all the three surfaces are faster than Mg(0001) system. Especially for the $Mg_{17}Al_{12}$(110) system, its dissociation barrier is 0.59 eV, which is significantly lowered compared to the Mg(0001) system of 0.84 eV.

Interestingly, analysis of the electronic properties explains the role of Al in faster hydrogen adsorption kinetics on $Mg_{17}Al_{12}$ surfaces. The differential charge density shows that there is a significant charge transfer from Mg to Al in the $Mg_{17}Al_{12}$ system. However, the H atoms of (110) and Mg(0001) gain about the same value of charges in TS and FS, which may lead to a stronger bonding between the H and the surface of the former. PDOS shows that the position of the H 1*s* orbit in both $Mg_{17}Al_{12}$ and pure Mg systems have a significant negative

shift during the transition from IS to TS, and finally shifts positively toward back from the TS to FS. Moreover, the main peaks of Al 3s orbitals are closer to H 1s, which facilitates the overlap of Al 3s and H 1s orbitals. This explains why the hydrogen dissociation barrier energies of the MEPs of the three $Mg_{17}Al_{12}$ systems are all lower than Mg(0001) system.

Declaration of competing interest

The authors declare that they have no known competing financial interests or personal relationships that could have appeared to influence the work reported in this paper.

Acknowledgements

This work is financially supported by the National Natural Science Foundation of China (No. 51621001 and 12074126), Natural Science Foundation of Guangdong Province of China (No. 2016A030312011), and Key Research and Development Project of Guangdong Province under Grant No. 2020B0303300001. The computing resources from the National Supercomputing Center in Guangzhou (NSCCGZ) are gratefully acknowledged.

REFERENCES

[1] Schlapbach L, Zuttel A. Hydrogen-storage materials for mobile applications. Nature 2001;414:353–8. https://doi.org/10.1038/35104634.

[2] Satyapal S, Petrovic J, Read C, Thomas G, Ordaz G. The US department of energy's national hydrogen storage Project: progress towards meeting hydrogen-powered vehicle requirements. Catal Today 2007;120:246–56. https://doi.org/10.1016/j.cattod.2006.09.022.

[3] Lai Q, Paskevicius M, Sheppard DA, Buckley CE, Thornton AW, Hill MR, et al. Hydrogen storage materials for mobile and stationary applications: current state of the art. ChemSusChem 2015;8:2789–825. https://doi.org/10.1002/cssc.201500231.

[4] Zuttel A. Hydrogen storage methods. Naturwissenschaften 2004;91:157–72. https://doi.org/10.1007/s00114-004-0516-x.

[5] Chen P, Zhu M. Recent progress in hydrogen storage. Mater Today 2008;11:36–43. https://doi.org/10.1016/s1369-7021(08)70251-7.

[6] Eberle U, Felderhoff M, Schueth F. Chemical and physical solutions for hydrogen storage. Angew Chem, Int Ed 2009;48:6608–30. https://doi.org/10.1002/anie.200806293.

[7] Dalebrook AF, Gan W, Grasemann M, Moret S, Laurenczy G. Hydrogen storage: beyond conventional methods. Chem Commun 2013;49:8735–51. https://doi.org/10.1039/c3cc43836h.

[8] Durbin DJ, Malardier-Jugroot C. Review of hydrogen storage techniques for on board vehicle applications. Int J Hydrogen Energy 2013;38:14595–617. https://doi.org/10.1016/j.ijhydene.2013.07.058.

[9] Abdalla AM, Hossain S, Nisfindy OB, Azad AT, Dawood M, Azad AK. Hydrogen production, storage, transportation and key challenges with applications: a review. Energy Convers Manag 2018;165:602–27. https://doi.org/10.1016/j.enconman.2018.03.088.

[10] Abe JO, Popoola API, Ajenifuja E, Popoola OM. Hydrogen energy, economy and storage: review and recommendation. Int J Hydrogen Energy 2019;44:15072–86. https://doi.org/10.1016/j.ijhydene.2019.04.068.

[11] Yartys VA, Lototskyy MV, Akiba E, Albert R, Antonov VE, Ares JR, et al. Magnesium based materials for hydrogen based energy storage: past, present and future. Int J Hydrogen Energy 2019;44:7809–59. https://doi.org/10.1016/j.ijhydene.2018.12.212.

[12] Shang CX, Bououdina M, Song Y, Guo ZX. Mechanical alloying and electronic simulations of (MgH_2 + M) systems (M=Al, Ti, Fe, Ni, Cu and Nb) for hydrogen storage. Int J Hydrogen Energy 2004;29:73–80. https://doi.org/10.1016/s0360-3199(03)00045-4.

[13] Vajo JJ, Mertens F, Ahn CC, Bowman RC, Fultz B. Altering hydrogen storage properties by hydride destabilization through alloy formation: LiH and MgH_2 destabilized with Si. J Phys Chem B 2004;108:13977–83. https://doi.org/10.1021/jp040060h.

[14] Hanada N, Ichikawa T, Fujii H. Catalytic effect of nanoparticle 3d-transition metals on hydrogen storage properties in magnesium hydride MgH_2 prepared by mechanical milling. J Phys Chem B 2005;109:7188–94. https://doi.org/10.1021/jp044576c.

[15] Imamura H, Hashimoto Y, Aoki T, Ushijima T, Sakata Y. Preparation and properties of ball-milled MgH_2/Al nanocomposites for hydrogen storage. Mater Trans 2014;55:572–6. https://doi.org/10.2320/matertrans.M2013368.

[16] Lu H, Li J, Lu Y, Chen Ya, Xie T, Zhou X, et al. ZrO_2@Nb_2CT composite as the efficient catalyst for Mg/MgH_2 based reversible hydrogen storage material. Int J Hydrogen Energy 2022;47:38282–94. https://doi.org/10.1016/j.ijhydene.2022.09.013.

[17] Liu M, Xiao X, Zhao S, Saremi-Yarahmadi S, Chen M, Zheng J, et al. ZIF-67 derived Co@CNTs nanoparticles: remarkably improved hydrogen storage properties of MgH_2 and synergetic catalysis mechanism. Int J Hydrogen Energy 2019;44:1059–69. https://doi.org/10.1016/j.ijhydene.2018.11.078.

[18] Dan L, Hu L, Wang H, Zhu M. Excellent catalysis of MoO_3 on the hydrogen sorption of MgH_2. Int J Hydrogen Energy 2019;44:29249–54. https://doi.org/10.1016/j.ijhydene.2019.01.285.

[19] Yahya MS, Sulaiman NN, Mustafa NS, Halim Yap FA, Ismail M. Improvement of hydrogen storage properties in MgH_2 catalysed by K_2NbF_7. Int J Hydrogen Energy 2018;43:14532–40. https://doi.org/10.1016/j.ijhydene.2018.05.157.

[20] Bouaricha S, Dodelet JP, Guay D, Huot J, Boily S, Schulz R. Hydriding behavior of Mg–Al and leached Mg–Al compounds prepared by high-energy ball-milling. J Alloys Compd 2000;297:282–93. https://doi.org/10.1016/s0925-8388(99)00612-x.

[21] Bououdina M, Guo ZX. Comparative study of mechanical alloying of (Mg+Al) and (Mg+Al+Ni) mixtures for hydrogen storage. J Alloys Compd 2002;336:222–31. https://doi.org/10.1016/S0925-8388(01)01856-4.

[22] Crivello JC, Nobuki T, Kato S, Abe M, Kuji T. Hydrogen absorption properties of the γ-$Mg_{17}Al_{12}$ phase and its Al-richer domain. J Alloys Compd 2007;446–447:157–61. https://doi.org/10.1016/j.jallcom.2006.12.055.

[23] Crivello JC, Nobuki T, Kuji T. Limits of the Mg–Al γ-phase range by ball-milling. Intermetallics 2007;15:1432–7. https://doi.org/10.1016/j.intermet.2007.05.001.

[24] Yabe H, Kuji T. Thermal stability and hydrogen absorption/desorption properties of $Mg_{17}Al_{12}$ produced by bulk mechanical alloying. J Alloys Compd 2007;433:241–5. https://doi.org/10.1016/j.jallcom.2006.06.043.

[25] Andreasen A. Hydrogenation properties of Mg–Al alloys. Int J Hydrogen Energy 2008;33:7489–97. https://doi.org/10.1016/j.ijhydene.2008.09.095.
[26] Crivello JC, Nobuki T, Kuji T. Improvement of Mg–Al alloys for hydrogen storage applications. Int J Hydrogen Energy 2009;34:1937–43. https://doi.org/10.1016/j.ijhydene.2008.11.039.
[27] Tanniru M, Ebrahimi F. Effect of Al on the hydrogenation characteristics of nanocrystalline Mg powder. Int J Hydrogen Energy 2009;34:7714–23. https://doi.org/10.1016/j.ijhydene.2009.06.078.
[28] Zhong HC, Wang H, Ouyang LZ. Improving the hydrogen storage properties of MgH_2 by reversibly forming Mg–Al solid solution alloys. Int J Hydrogen Energy 2014;39:3320–6. https://doi.org/10.1016/j.ijhydene.2013.12.074.
[29] Lu W-C, Ou S-F, Lin M-H, Wong M-F. Hydrogen absorption/desorption performance of Mg-Al alloys synthesized by reactive mechanical milling and hydrogen pulverization. J Alloys Compd 2016;682:318–25. https://doi.org/10.1016/j.jallcom.2016.04.236.
[30] Peng W, Lan Z, Wei W, Xu L, Guo J. Investigation on preparation and hydrogen storage performance of $Mg_{17}Al_{12}$ alloy. Int J Hydrogen Energy 2016;41:1759–65. https://doi.org/10.1016/j.ijhydene.2015.11.138.
[31] Li Y, Zhang Y, Shang H, Qi Y, Li P, Zhao D. Investigation on structure and hydrogen storage performance of as-milled and cast $Mg_{90}Al_{10}$ alloys. Int J Hydrogen Energy 2018;43:6642–53. https://doi.org/10.1016/j.ijhydene.2018.02.086.
[32] Jang HS, Kang HJ, Yoon P, Lee G, Jeon JB, Park JY, et al. Effects of Mg content on hydrogen content and melt quality of Al-Mg alloys. Metals 2019;9. https://doi.org/10.3390/met9111235.
[33] Dai JH, Song Y, Yang R. Intrinsic mechanisms on enhancement of hydrogen desorption from MgH_2 by (001) surface doping. Int J Hydrogen Energy 2011;36:12939–49. https://doi.org/10.1016/j.ijhydene.2011.07.062.
[34] Kelkar T, Pal S, Kanhere DG. Density functional investigations of electronics structure and dehydrogenation reactions of Al- and Si-substituted magnesium hydride. ChemPhysChem 2008;9:928–34. https://doi.org/10.1002/cphc.200700860.
[35] Zaluska A, Zaluski L, Strom-Olsen JO. Nanocrystalline magnesium for hydrogen storage. J Alloys Compd 1999;288:217–25. https://doi.org/10.1016/s0925-8388(99)00073-0.
[36] Kresse G, Furthmüller J. Efficient iterative schemes for ab initio total-energy calculations using a plane-wave basis set. Phys Rev B 1996;54:11169–86. https://doi.org/10.1103/PhysRevB.54.11169.
[37] Perdew JP, Chevary JA, Vosko SH, Jackson KA, Pederson MR, Singh DJ, et al. Atoms, molecules, solids, and surfaces: applications of the generalized gradient approximation for exchange and correlation. Phys Rev B 1992;46:6671–87. https://doi.org/10.1103/PhysRevB.46.6671.
[38] Perdew JP, Burke K, Ernzerhof M. Generalized gradient approximation made simple. Phys Rev Lett 1996;77:3865–8. https://doi.org/10.1103/PhysRevLett.77.3865.
[39] Monkhorst HJ, Pack JD. Special points for Brillouin-zone integrations. Phys Rev B 1976;13:5188–92. https://doi.org/10.1103/PhysRevB.13.5188.
[40] Henkelman G, Uberuaga BP, Jonsson H. A climbing image nudged elastic band method for finding saddle points and minimum energy paths. J Chem Phys 2000;113:9901–4. https://doi.org/10.1063/1.1329672.
[41] Huang M-X, Liu F, He C-C, Yang S-Q, Chen W-Y, Ouyang L, et al. Interface promoted CO_2 methanation: a theoretical study of Ni/La_2O_3. Chem Phys Lett 2021;768. https://doi.org/10.1016/j.cplett.2021.138396.
[42] Chen W-Y, Tang J-J, Lu Z-W, Huang M-X, Liu L, He C-C, et al. Theoretical investigation of the surface orientation impact on the hydrogen vacancy formation of MgH2. Surf Sci 2021:710. https://doi.org/10.1016/j.susc.2021.121850.
[43] Singh D, Suryanarayana C, Mertus L, Chen RH. Extended homogeneity range of intermetallic phases in mechanically alloyed Mg–Al alloys. Intermetallics 2003;11:373–6. https://doi.org/10.1016/s0966-9795(03)00005-0.
[44] Pozzo M, Alfe D. The role of steps in the dissociation of H_2 on Mg(0001). J Phys Condens Matter 2009;21:095004. https://doi.org/10.1088/0953-8984/21/9/095004.
[45] Li Y, Yang Y, Wei Y, Zhang P. Influences of Al doping on the electronic structure of Mg(0001) and dissociation properties of H_2. Phys Lett 2010;374:975–80. https://doi.org/10.1016/j.physleta.2009.12.011.
[46] Dai JH, Song Y, Shi B, Yang R. First-principles study on a potential hydrogen storage medium of Mg/TiAl sandwiched films. J Phys Chem C 2013;117:25374–80. https://doi.org/10.1021/jp409706r.
[47] Pozzo M, Alfe D, Amieiro A, French S, Pratt A. Hydrogen dissociation and diffusion on Ni- and Ti-doped Mg(0001) surfaces. J Chem Phys 2008;128. https://doi.org/10.1063/1.2835541.